Power gain optimization for far user performance enhancement in multiview video transmission over NOMA system

DOI: 10.5281/zenodo.6991791

Ali Mohammed Hasan
University of Tikrit, College of Engineering, Tikrit, Iraq.
ali.m.hassan43853@st.tu.edu.iq

Ibrahim Khalil Sileh
University of Tikrit, College of Engineering, Tikrit, Iraq.
ibrahimks65@tu.edu.iq

Abstract

Non-orthogonal multiple access (NOMA), which has just been proposed, may be more spectrally efficient than conventional orthogonal multiple access. Although it is currently challenging to provide, high performance video streaming has the potential to satisfy the growing demand for video services. For the first time, we study a multi-user NOMA system design in this work for video transmission. There have been several NOMA methods for data transfer that have been suggested, each with a different throughput or dependability. The user's perceived quality, or quality of experience, is crucial for video transmission. Based on this discovery, we create a cross-layer, multi-user, quality-driven, scalable, video transmission system with support for NOMA. To enable low complexity multi-user NOMA procedures, an innovative user grouping technique is provided. The primary elements of the suggested framework are the conception of multi-user NOMA-based video transmission as a quality-driven power allocation problem and the integration of the encoded video quality model with the physical layer model for NOMA transmission. Due to the non-concavity of the problem, two strategies are created: a global optimal strategy based on the hidden monotonic requirement and a suboptimal strategy with polynomial time complexity. According to simulation results, the proposed multi-user NOMA system outperforms existing techniques in a range of video distribution scenarios.

Introduction

Due to the increasing rise of mobile data traffic, new multiple access techniques have been developed to address the demand for high spectrum and energy efficiency, low latency, and good quality of service (QoS) in 5G wireless communication systems [1]. Due to the fact that the orthogonal frequency division multiple access (OFDMA) network is based on frequency allocation, where each resource block is allocated to a single user at each time slot, the main challenges of using OFDMA in the 5G networks are QoS and interference management for a large number of users [2,3]. Non-Orthogonal Multiple Access (NOMA), one method to address the issues of 5G networks and beyond, has recently received increased attention from researchers [4]. The NOMA system, which enables several users to simultaneously share the same frequency channel, has several benefits, including spectrum efficiency and fairness between base station (BS)-close and edge users [5]. To be more precise, NOMA leverages this cutting-edge resource allocation technique to get beyond OFDMA networks' frequency restrictions. Two broad categories for NOMA systems are the code-domain NOMA (C-NOMA) and power-domain NOMA (P-NOMA) classes [6]. The P-NOMA system organises the power distribution of users in accordance with the channel's state, which is determined by the channel's bandwidth, fading channel gain, noise power, and transmission data rate. Additionally, despite taking into account a different weighted coefficient factor for each user, it distributes the same subchannel among numerous users. In order to achieve the power distribution of the P-NOMA scheme, the channel

state information (CSI) and another element are merged [7]. The NOMA system divides the signals of multiple users and delivers distinct signals concurrently to a large number of receivers using superposition-coding (SC) at the transmitter and sequential interference cancellation (SIC) [8] at the receiver. Because P-NOMA divides user entities by sending powers in the same subchannel, interuser interference (IUI) significantly increases the bit error rate (BER) [9]. Although there are several benefits to using NOMA in various wireless networks, one of the main challenges to its effective application in modern wireless systems is the SIC method. This is a result of the intricate decoding algorithm and error propagation used by the NOMA system [10]. Therefore, using a shared frequency sub-channel without any SIC augmentation would not be a good idea because the inaccuracy increases proportionally with the number of users. This issue could worsen in the upcoming generation of wireless networks, known as ultra-dense heterogeneous networks [11], when more smart devices equipped with NOMA techniques are used in congested areas. Furthermore, 5G networks will employ millimeter-wave frequency ranges. This approach causes more out-of-band distortion at the non-linear area of the power amplifiers (PAs) than the previous generation did [12]. The orthogonal frequency division multiplexing (OFDM)-based NOMA system [13] has drawn a lot of attention in contrast to other popular NOMA systems because of its capacity to boost spectrum efficiency. In this paper, power NOMA based on various power gains is implemented for transmitting a Multiview video. Performance of the proposed system is examined when video transmission is performed between two users unequally separated from the base station.

Multiview Video Preparation

Video Decoding

A 3D video system's two elements are depth and colour. High-quality 3D video is more beautiful and lifelike than 2D video because it provides the viewer a sense of depth (the third dimension). 3D video has recently drawn interest unlike anything other due to improvements in the recording, encoding, and projection technologies as well as their rapidly growing uses. The user of a 3D video system can see depth in the scene they are seeing. One can achieve such 3D depth perception by using specialised 3D display systems that allow people to analyse 3D visual information with both eyes . A few formats for 3D video footage include Multi-View Video (MVV), Video plus Depth (V+D), and Traditional Stereo Video (CSV). Since different 3D video formats can be represented by different coding and compression techniques The substantial amount of data generated by the depth map produced by the 3D video, which must be transported or stored, makes the process of transmitting 3D video more challenging. This activity involved the recording, encoding, transmission, and presentation of 3D video through several processing phases. Aspects of video compression include the use of spatial, temporal, and bit stream redundancy as well as the elimination of high-frequency components. There are many different data formats produced by various 3D content production processes. The available 3D video formats, including Multi-View Video plus Depth (MV+D), Conventional Stereo Video (CSV), and Video plus Depth (V+D), are all described in . These formats are encoded using the H.264/AVC industry standard for advanced video coding, which employs several techniques for 3D video encoding and decoding. The Video plus Depth (V+D) format will be used in this inquiry. We'll also give a quick overview of the relevant coding techniques for video compression using H.264/AVC, transmission over a Rayleigh fading channel, and video decompression using the same H.264/AVC to get to the end user.

Video Transmission

Video data are being prepared as 3D video is processed through the algorithm below where frames with same size are extracted. Hence after, frames are being transmitted over NOMA system through fading channel. Firstly, 3D video is slotted with same length frames in such way if the frames are seen sequentially then it will yield the same original video.

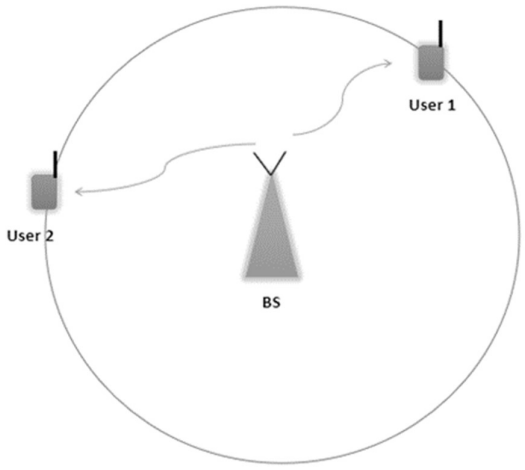

Figure 1: User-base station depicts the distance between the used and base station.

As seen in Figure 1, the system is modulated, with the base station at the heart of the network arena and two users connecting to it using the NOMA technique. Table 1 contains system configurations. A Multiview video clip of 64 seconds in length must be broadcast using the system that meets the requirements listed in Table 1. First, this video is divided into a series of frames, with each frame being represented by an x and y amount of pixels, where x stands for frame width and y represents for frame height. This video is then delivered through AWGN and Rayleigh fading channels. In order to examine the model performance, four scenarios are made using different power gains see Table 1.

Table 1: NOMA model configurations and proposed seniors.

Particle	Details
Number of users	Two (2)
Distance from base station (user 1)	1000 m
Distance from base station (user 2)	500 m
Power weights Scenario 1	0.55, 0.45
Power weights Scenario 2	0.60, 0.40
Power weights Scenario 3	0.70, 0.30
Power weights Scenario 4	0.80, 0.20
Modulation	BPSK
Channel	AWGN, Rayleigh Fading
SNR	(0-30 dB)

BER and MSE

Bit error rate (BER) of the far user is see enhanced if the power gain of that user increased see Figure 2. Mean square error (MSE) for the video data transmitted is measured according to the equation (2). First of all, error is calculated by comparing the received data and original data, however, applying MSE formula is being done on the calculated error.

$$E = D - T \quad (1)$$

$$MSE = \sum_{n=1}^{N} E[n]^2 \quad (2)$$

Where E is the error vector, D is the original transmitted data at the transmitter end, T is the received data at the receiver end, both the transmitted data and received data are of length N. MSE is higher for the far user with lesser power gain and it can be decreased if power gain increased (see Figure 3, Table 2).

Figure 2: Bit error rate vs SNR demonstration in every scenario.

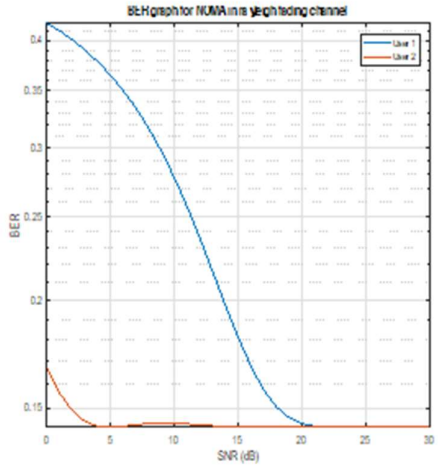

Scenario 1

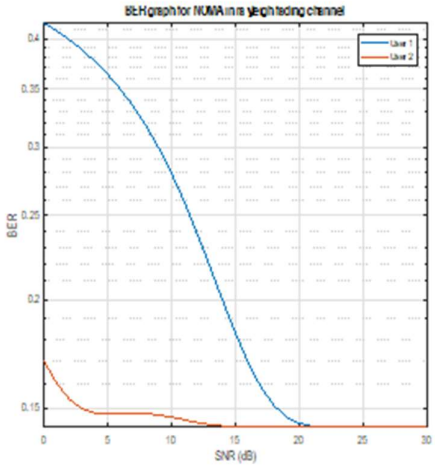

Scenario 2

Scenario 1

Scenario 2

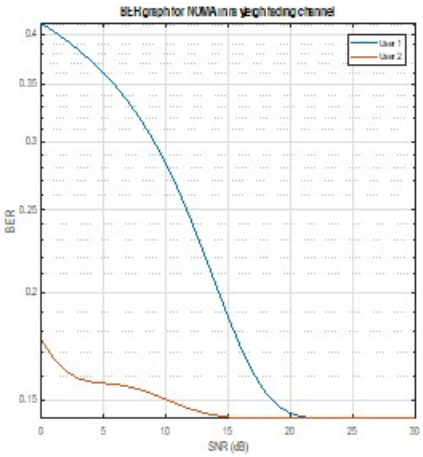

Scenario 3

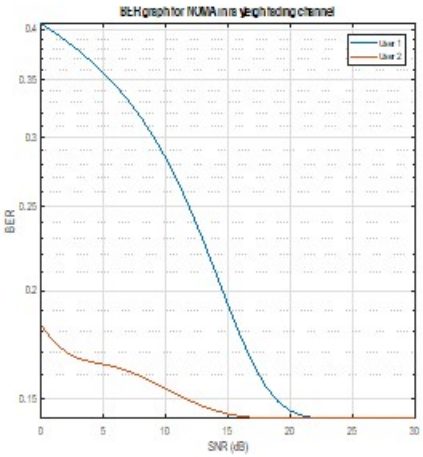

Scenario 4

Table 2: mean value of mean square errors calculated for each user in every senior.

---	Senior 1	Senior 2	Senior 3	Senior 4
Mse user 1	0.2767	1.2416	0.3742	0.8235
Mse user 2	0.0969	0.2545	0.3753	1.0544

Results tabulated in Table 2 can be graphically demonstrated at Figure below:

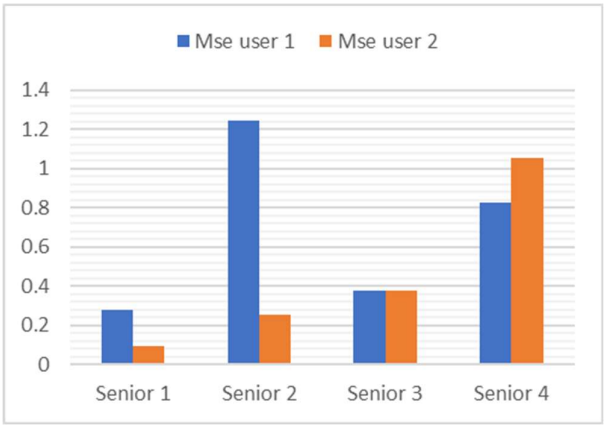

Figure 3: Mean square error comparison of both users.

PSNR

The transmitted video is being undergoing Rayleigh fading channel so the video data at the received end is being doped with noise that is leading to pixels error. The pixel to noise ration per video frame is calculated for both first and second users and can be demonstrated in Figure below. Results shown that pixel to noise ratio is higher in the user 1 (far user) when the power gain of this user is 0.55 and the power gain for the other user (near user) is 0.45. On the other hand, pixel to noise ratio in the far user is continued to be high when the power gain increased in Scenario 2 e.g. (far user power gin is 0.60 and near user power gain is 0.40). however, if the power gain of far user is more increased as in scenario 3 and scenario 4, the pixel to noise ration will be decreased for this user (see Figure 4).

Figure 4: PSNR per frame per user of the received data.

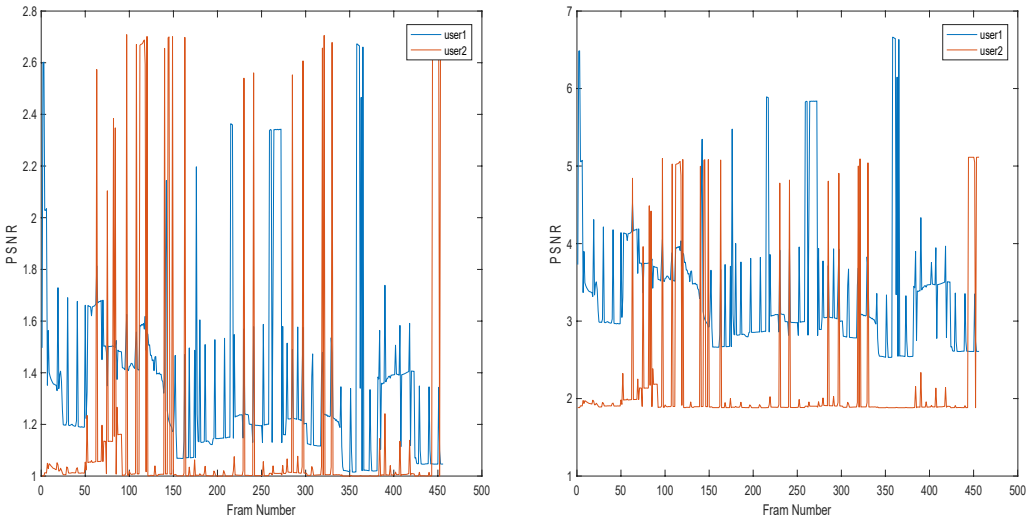

Scenario 1 Scenario 2

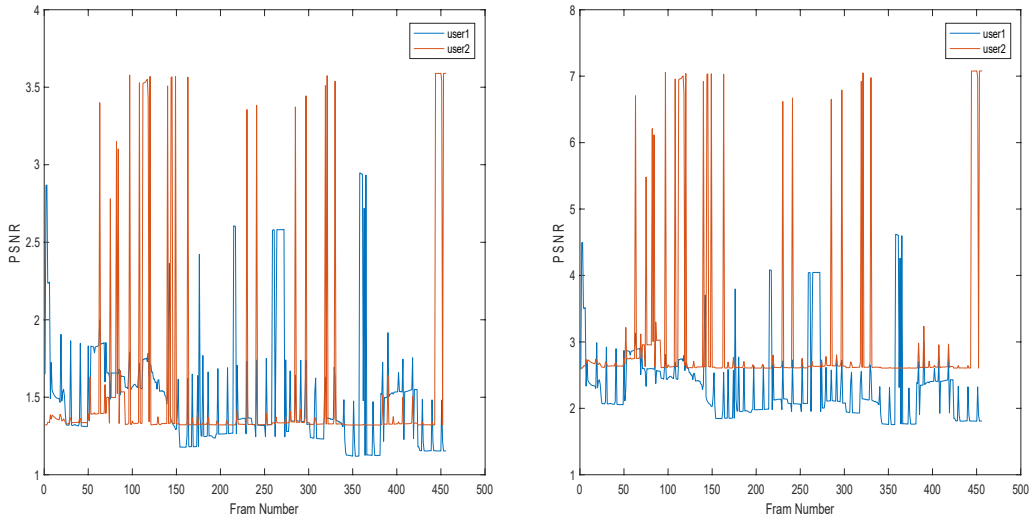

Scenario 3 Scenario 4

Channel Performance

In order to evaluate the channel performance two metrics are calculated namely outage probability and channel capacity which are demonstrated in Figures (5 and 6). Outage probability is showing that far user at scenario 1 when relatively near values of power gains for the user1 and user 2 are assigned that user 1 (the far user) has outage probability greater than user 2 which means that user 1 has not achieved the targeted PSNR. When the power gain of the far user is being increased, as in scenario 3 and scenario 4, outage probability is intern decreased.

Figure 4: outage probability vs transmitted power per user of the received data.

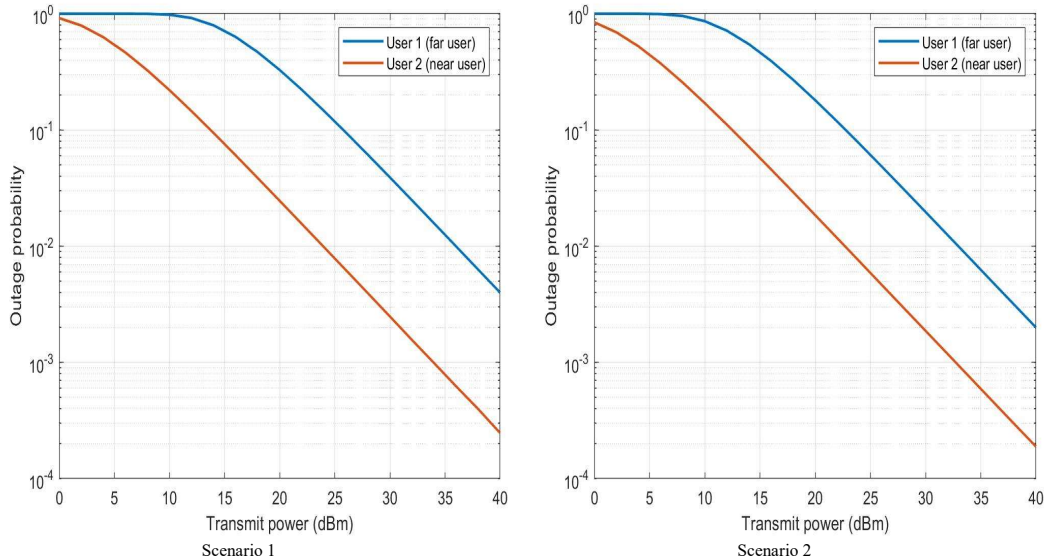

Scenario 1 Scenario 2

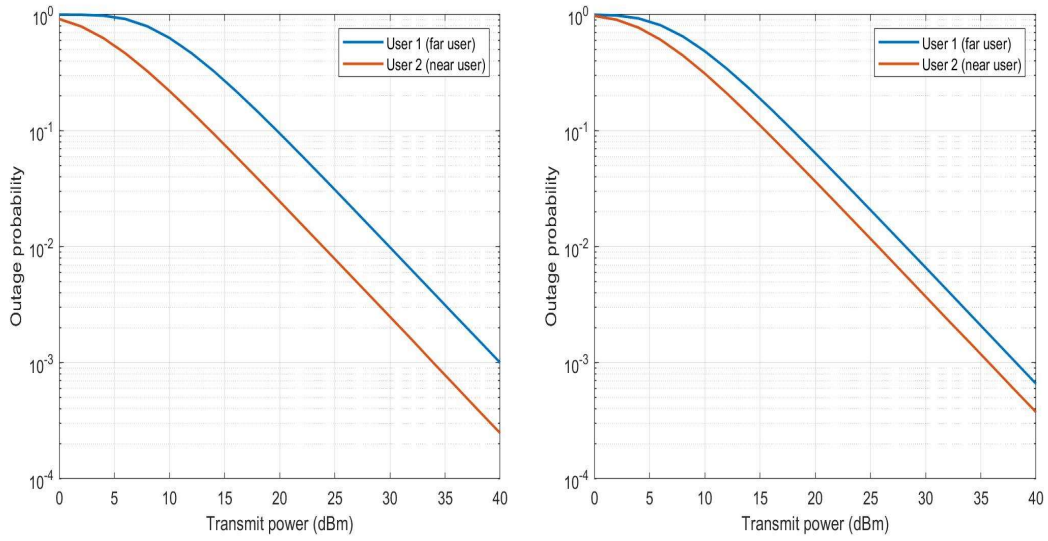

Scenario 3 Scenario 4

Channel capacity is being monitored within the proposed power gains variations (scenarios). Three channels are detected which is represented by R1: the channel between the user 1 and base station, R2: the channel between the user 2 and base station, R12: the channel between the user 1 and the user 2. Figure below () shows that channel capacity of the near user (user 2) is greater than that in the far user (user 1), however, when power gain of the far user was increased, we realized that channel capacity if this user and base station is also increased. However, the channel capacity of the channel between user 1 and user 2 is remained constant in all proposed scenarios.

Figure 5: channel capacity vs transmitted power per user of the received data.

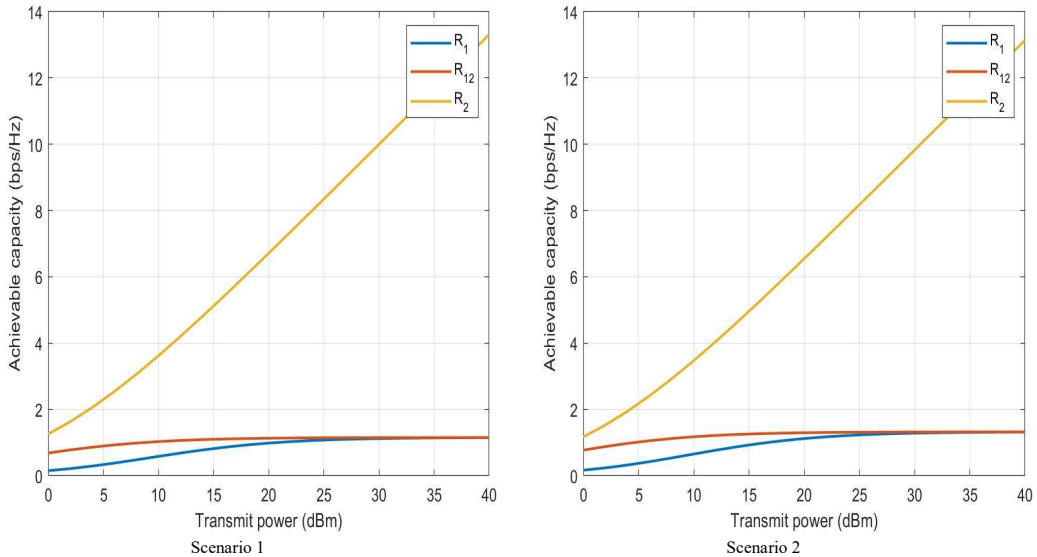

Scenario 1 Scenario 2

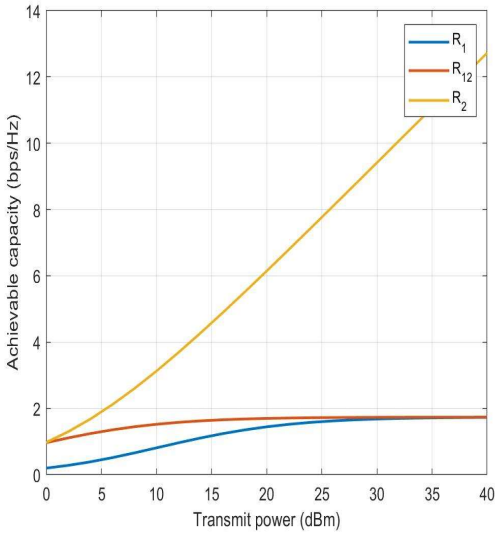

Scenario 3

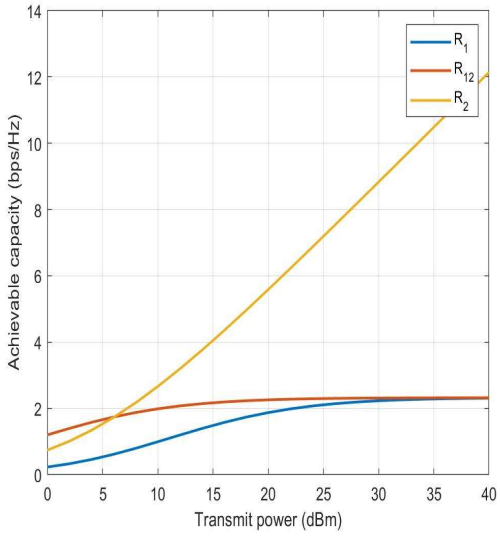

Scenario 4

Conclusion

Multi view video transmission using NOMA system over Rayleigh fading and AWGN channel is challengeable task due to the uncountable noise impact. This noise in impacting video quality and degrading the system performance. In this paper, NOMA system is being examined for the mentioned channel noise by monitoring the impact of power gains of both users on battery of metrics including BER, MSE, PSNR as well as channel performance metrics. Far user is getting direct impact by the channel disturbances i.e. noise as demonstrated above. It is realized that bit error rate as well as mean square error and PSNR is on the higher side in case of far user while it is moderated for the near user. Channel impact can be minimized by increasing the power gain of the far user so that the resultant metrics BER, MSE, PSNR as well as channel performance metrics will be moderated as the near user performance.

References

- Y. Liu, Y. Yang, P. Han, Z. Shao, and C. Li, "Virtual network embedding in fiber-wireless access networks for resource-efficient IoT service provisioning," IEEE Access, vol. 7, pp. 65506–65517, 2019.
- R. Boussada, B. Hamdane, M. E. Elhdhili, and L. A. Saidane, "Privacy-preserving aware data transmission for IoT-based e-health," Computer Networks, vol. 162, article 106866, 2019.
- Rachedi, M. H. Rehmani, S. Cherkaoui, and J. J. P. C. Rodrigues, "IEEE access special section editorial: the plethora of research in Internet of things (IoT)," IEEE Access, vol. 4, pp. 9575–9579, 2016.
- Z. Wang, J. Wang, Y. Zhang, and D. Niyato, "Strategic access and pricing in Internet of things (IoT) service with energy harvesting," IEEE Access, vol. 7, pp. 34655–34674, 2019.
- Musaddiq, Y. B. Zikria, O. Hahm, H. Yu, A. K. Bashir, and S. W. Kim, "A survey on resource management in IoT operating systems," IEEE Access, vol. 6, pp. 8459–8482, 2018.
- S. Popli, R. K. Jha, and S. Jain, "A survey on energy efficient narrowband Internet of things (NBIoT): architecture, application and challenges," IEEE Access, vol. 7, pp. 16739–16776, 2019.
- G. Han, L. Wan, J. J. P. C. Rodrigues, H. Wu, and D. Zhang, "IEEE access special section editorial: green communications and networking for 5G," IEEE Access, vol. 6, pp. 79263–79271, 2018.

- N. Panwar, S. Sharma, and A. K. Singh, "A survey on 5G: the next generation of mobile communication," Physical Communication, vol. 18, pp. 64–84, 2016.
- H. Ullah, N. Gopalakrishnan Nair, A. Moore, C. Nugent, P. Muschamp, and M. Cuevas, "5G communication: an overview of vehicle-to-everything, drones, and healthcare use-cases," IEEE Access, vol. 7, pp. 37251–37268, 2019.
- G. J. Foschini and Z. Miljanic, "A simple distributed autonomous power control algorithm and its convergence," IEEE Transactions on Vehicular Technology, vol. 42, no. 4, pp. 641–646, 1993.
- S. Gupta, R. D. Yates, and C. Rose, "Soft dropping power control - a power control backoff strategy," in IEEE International Conference on Personal Wireless Communications, pp. 210–214, Mumbai, India, India, Dec. 1997.
- M. G. d. S. Rêgo, T. F. Maciel, H. d. H. M. Barros, F. R. P. Cavalcanti, and G. Fodor, "Performance analysis of power control for device-to-device communication in cellular MIMO systems," in International Symposium on Wireless Communication Systems, pp. 336–340, Paris, France, Aug. 2012.
- S. Buzzi and D. Saturnino, "A game-theoretic approach to energy efficient power control and receiver design in cognitive CDMA wireless networks," IEEE Journal of Selected Topics in Signal Processing, vol. 5, no. 1, pp. 137–150, 2011.